Optimization of Axially Magnetized Stack Structured Permanent Magnet Thrust Bearing Using Three-Dimensional Mathematical Model

Siddappa I. Bekinal[1]
Bearings Laboratory,
Department of Mechanical Engineering,
KLS Gogte Institute of Technology,
Belagavi 590008, Karnataka, India
e-mail: sibekinal@git.edu

Mrityunjay Doddamani
Department of Mechanical Engineering,
National Institute of Technology Karnataka,
Surathkal 575025, Karnataka, India
e-mail: mrdoddamani@nitk.edu.in

Soumendu Jana
Bearings and Rotor Dynamics Laboratory,
Propulsion Division,
National Aerospace Laboratories,
Bengaluru 560017, Karnataka, India
e-mail: sjana@nal.res.in

*This work deals with optimization of axially magnetized stack structured permanent magnet (PM) thrust bearing using generalized three-dimensional (3D) mathematical model having "*n*" number of ring pairs. The stack structured PM thrust bearing is optimized for the maximum axial force and stiffness in a given cylindrical volume.* MATLAB *codes are written to solve the developed equations for optimization of geometrical parameters (axial offset, number of ring pairs, air gap, and inner radius of inner and outer rings). Further, the results of proposed optimization method are validated using finite element analysis (FEA) and further, generalized by establishing the relationship between optimal design variables and air gap pertaining to cylindrical volume constraint of bearing's outer diameter. Effectiveness of the proposed method is demonstrated by optimizing PM thrust bearing in a given cylindrical volume. Mathematical model with optimized geometrical parameters dealt in the present work helps the designer in developing PM thrust bearings effectively and efficiently for variety of applications.* [DOI: 10.1115/1.4034533]

Introduction

High-speed applications [1–3] demand for optimal design and selection of bearings for contactless drive, zero maintenance, higher reliability, lower vibration, and reduced noise levels. Passive magnetic bearings (PMBs) are the potential devices addressing these issues effectively and efficiently. These bearings are realized by arranging axially and/or radially magnetized PM rings [4–6]. In the recent past, researchers elaborately discussed force and stiffness characteristics of PM bearing with one ring pair with two-dimensional (2D) analytical [7] or 3D semi-analytical [8–11] equations using Coulombian or Amperian approaches. Yonnet et al. [12] addressed low stiffness or force associated with PM bearing with single ring pair by stacking the rings in alternate oppositions. Further, 2D analytical equations for force and stiffness in stack structured PM bearing configurations with *n* number of ring pairs are presented [13,14]. Though, 2D equations are simple to deal with reduced computational time, they lack precision [15–17] due to undermining curvature effect. This fact necessitates development of generalized 3D mathematical model in standard configurations of PM bearing with *n* number of ring pairs [18]. The stack structured PM bearings might replace conventional ball bearings or can be used in weight compensated high-speed applications requiring optimization for maximum force or stiffness in a given cylindrical volume. Lijesh and Hirani [19] have presented the optimization of radial axial polarized PMB with one ring pair for maximum load carrying capacity within minimum magnet volume. In this, optimization technique is used for lower stiffness or force with one ring pair. Optimization of repulsive passive magnetic bearings for maximum radial stiffness was presented by Moser et al. [20] using 2D FEA. Two-dimensional mathematical model to optimize the stack structured noncontact thrust bearing for maximum axial force with minimum magnet volume is discussed by Yoo et al. [21]. Studies on optimizing the stack structured PM bearings are limited to, either 2D FEA or mathematical expressions lacking precision as against 3D mathematical equations.

This work deals with modification and generalization of earlier presented 3D mathematical model [18] developed for axially, radially, and perpendicularly magnetized PMB's with *n* number of ring pairs. Mathematical expressions developed in Ref. [18] are generalized for axially magnetized stack structured PM thrust bearing and utilized for the optimization for maximum axial force and stiffness in a given cylindrical volume. MATLAB codes are developed to solve 3D equations to carry out the optimization for axial offset, number of ring pairs, air gap, and inner radius of inner and outer rings. Results from the mathematical model are compared with FEA and found to be in close agreement. Generalized method representing the relationship between optimized design variables and air gap for outer diameter of the bearing is also presented. Finally, the generalized plots are used to optimize the PM thrust bearing.

Permanent Magnet Thrust Bearing Configurations

The axially magnetized PM thrust bearing configurations with one ring pair (Fig. 1(*a*)) and stack structured configuration (Fig. 1(*b*)) in a given cylindrical volume with geometrical dimensions are presented in Fig. 1. The design variables considered for maximization of axial force and stiffness are axial offset (z), number of ring pairs (n), inner radius of inner rings ($R1$), inner radius of outer rings ($R3$), and air gap (g). The optimum values of these design variables at which axial force and stiffness are maximum are estimated using 3D mathematical model. The dimensions of PM thrust bearing with an aspect ratio (AR) ($L/2R4$) of 0.5 are

[1]Corresponding author.

Contributed by the Tribology Division of ASME for publication in the JOURNAL OF TRIBOLOGY. Manuscript received March 20, 2016; final manuscript received August 13, 2016; published online January 10, 2017. Assoc. Editor: Daejong Kim.

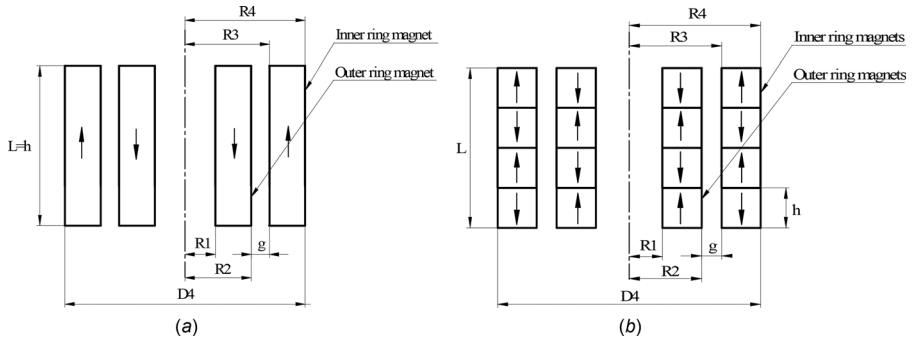

Fig. 1 PM thrust bearing configuration in a cylindrical volume with (*a*) one ring pair and (*b*) multiple ring pairs arranged in oppositions (stack-structured configuration)

Table 1 Parametric values of PM thrust bearing

Parameter	Value
Inner radius of inner rings, $R1$ (m)	0.009
Outer radius of inner rings, $R2$ (m)	0.014
Inner radius of outer rings, $R3$ (m)	0.015
Outer radius of bearing, $R4$ (m)	0.02
Air gap, g (m)	0.001
Axial length, L (m)	0.02
Magnetic polarization, $\mathbf{B_r}$ (T)	1.2
Aspect ratio, AR = $L/2R4$	0.5

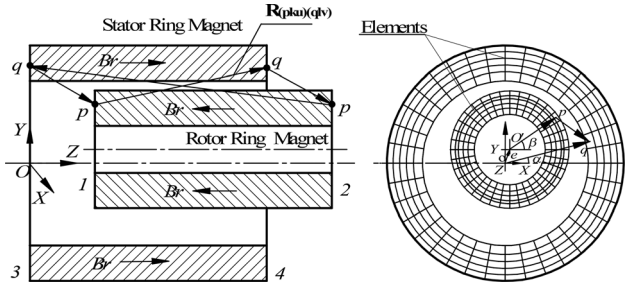

Fig. 2 Arrangement of *u*th and *v*th rings of PM thrust bearing

selected for the optimization. The parametric values chosen for optimizing the design variables are listed in Table 1.

Mathematical Model

In our earlier effort [18], generalized 3D mathematical models were developed to determine the force and stiffness in PM bearing for three standard configurations with n number ring pairs using the Colombian model and vector approach. In this work, an effort has been put in to generalize the mathematical model applicable to axially magnetized PM thrust bearing with n ring pairs to express a semi-analytical equation to estimate an axial force generated by outer rings on the inner one. The derived semi-analytical expression is utilized to carry out the optimization process. The uth PM ring fitted to the rotor and vth ring to stator is presented in Fig. 2. The rotor ring is unconstrained in x, y, and z directions with respect to the fixed outer ring. The inner and outer radii of the all-inner permanent magnet rings are $R1$ and $R2$, respectively. $R3$ and $R4$ are inner and outer radii of all-outer rings, respectively. Axial length of both inner and outer rings is h and radial thickness of all inner rings is equal to the radial thickness of all outer rings ($R2-R1=R4-R3$). The charged surfaces of rotor magnet ring are 1, 2 and 3, 4 represents stator magnet surfaces, respectively.

For PM thrust bearing with n number of axially polarized ring pairs arranged in opposition and "m" number of discrete surface elements on surfaces of rotor and stator, the resultant axial force in XYZ coordinate system is given by

$$F_Z = \frac{\mathbf{B_r^2}}{4\,\pi\,\mu_0}\sum_{u=1}^{n}\sum_{v=1}^{n}\sum_{k=1}^{2}\sum_{l=3}^{4}\sum_{p=1}^{m}\sum_{q=1}^{m}\frac{S_{pku}\,S_{qlv}}{R^3_{(pku)(qlv)}} \times \mathbf{R_{(pku)(qlv)}}\,(-1)^{(k+l)}\,(-1)^{(u+v)} \quad (1)$$

where the position vector, $\mathbf{R_{(pku)(qlv)}} = (X_{qlv}-X_{pku})\mathbf{i} + (Y_{qlv}-Y_{pku})\mathbf{j} + (Z_{qlv}-Z_{pku})\mathbf{k}$, S_{pku}—surface area of pth element located on kth surface of uth rotor ring, S_{qlv}—surface area of qth element located on lth surface of vth stator ring. The positions of the elements on the faces of uth ring pair in terms of the mean radius of the stator (r_{ms}) and rotor (r_{mr}) from the respective centers are expressed as

$$\begin{aligned} X_{pku} &= (x + r_{mr}\cos\beta)\,\mathbf{i} \quad X_{qlv} = (r_{ms}\cos\alpha)\,\mathbf{i} \\ Y_{pku} &= (y + r_{mr}\sin\beta)\,\mathbf{j} \quad Y_{qlv} = (r_{ms}\sin\alpha)\,\mathbf{j} \\ Z_{pku} &= (z + (u-1)\,l)\,\mathbf{k} \quad Z_{qlv} = (v\,l)\,\mathbf{k} \end{aligned} \quad (2)$$

where r_{mr} is the mean radius of pth element located on kth surface of uth rotor ring from its center "O′" and r_{ms} is the mean radius of qth element located on lth surface of vth stator ring from its center "O"

$$r_{mr} = R1 + (j-1)((R2-R1)/N1) + (R2-R1)/(2N1) \quad (3)$$

$$r_{ms} = R3 + (j-1)((R4-R3)/N1) + (R4-R3)/(2N1) \quad (4)$$

where $N1$ is the number of element divisions on the polarized surfaces of uth rotor and vth stator rings in the radial direction and $j = 1, 2, 3, \text{———}, N1$.

The axial stiffness generated in the stack-structured configuration is given by

$$K_z = \frac{dF_Z}{dZ} = \frac{1}{2\,\Delta Z}\left[F_Z(Z+\Delta Z) - F_Z(Z-\Delta Z)\right] \quad (5)$$

Equations (1) and (5) are coded in MATLAB to optimize the design variables for maximizing axial force and stiffness in a given cylindrical volume.

Optimization

Permanent magnet thrust bearings are designed to function at maximum axial force or stiffness in a given cylindrical volume. The design variables governing its functionality are axial offset, number of ring pairs, inner and outer radii of inner and outer rings, air gap and axial length of each ring pair. The following steps are followed in optimizing the design variables:

- Among all variables, $R4$ and L are fixed due to cylindrical volume constraint.

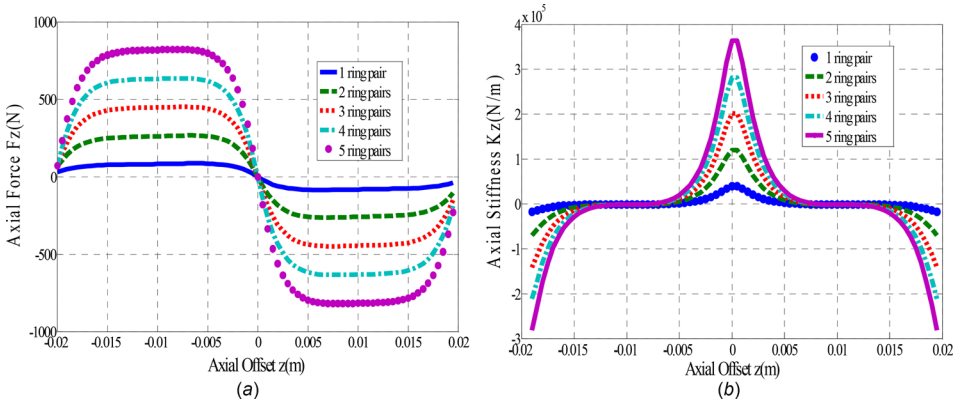

Fig. 3 Characteristics of stack structured PM thrust bearings with 1–5 ring pairs: $R1 = 0.009$ m, $R2 = 0.014$ m, $R3 = 0.015$ m, $R4 = 0.02$ m, $B_r = 1.2$ T, and $h = 0.02$ m (*a*) axial force and (*b*) axial stiffness

- Among others, variables that affect the bearing characteristics to the greater extent are axial offset (z), number of rings (n), and air gap (g) [18]. The effect of an axial offset is demonstrated by calculating the axial force and stiffness generated in the selected configuration (Table 1) using developed equations. The calculations are carried out by varying the number of ring pairs from one to five with 0.02 m ring axial length (h). The variations of axial force and stiffness with an axial offset are plotted in Fig. 3. From Fig. 3, it's clear that the force generated is maximum at an axial offset of

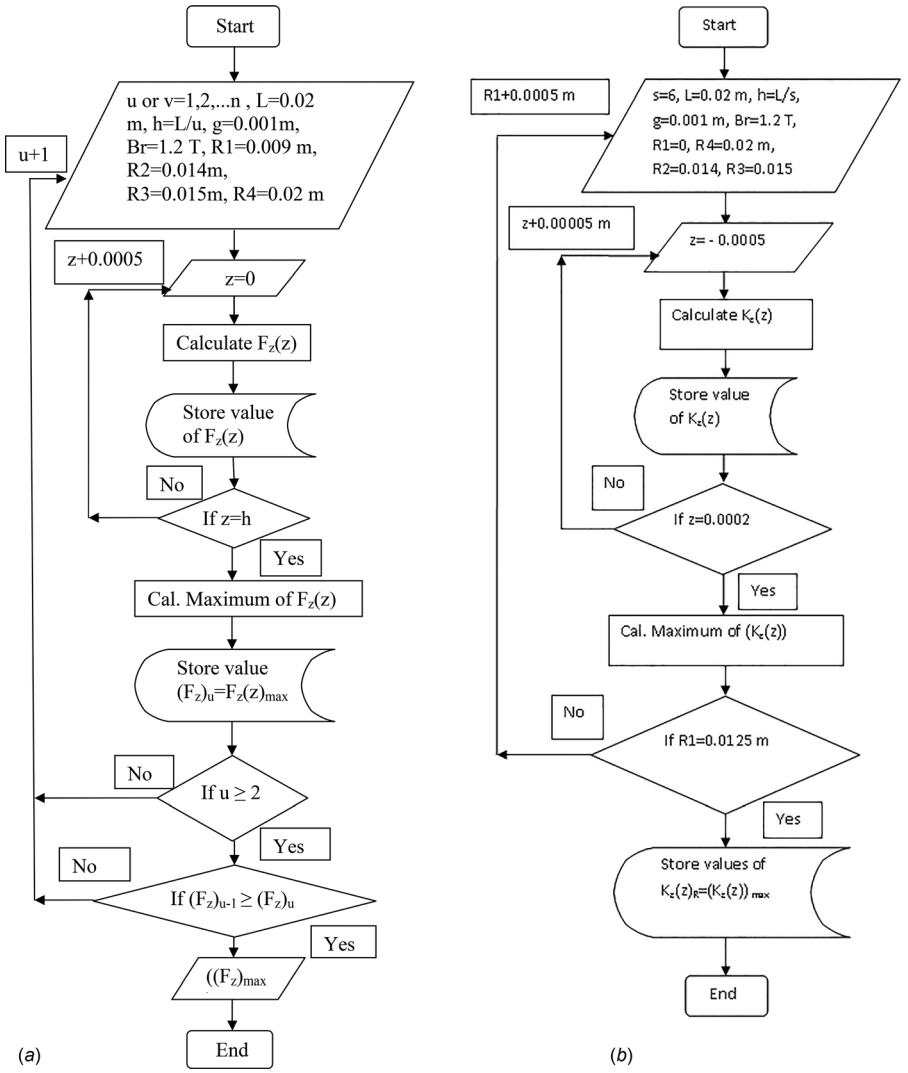

Fig. 4 Optimization of number of ring pairs for maximum (*a*) axial force and (*b*) optimization of $R1$ for maximum axial stiffness

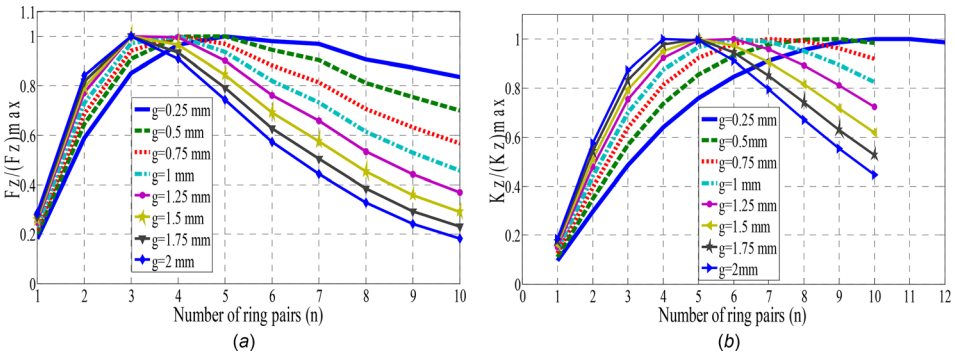

(*a*) (*b*)

Fig. 5 Variation of optimized values for number of ring pairs with varying air gap in maximum axial (*a*) force and (*b*) stiffness

Table 2 Optimized values for number of ring pairs

Air gap "g" (mm)	$(n)_{opt}$ for max. axial force	$(n)_{opt}$ for max. axial stiffness
0.25	5	11
0.5	5	9
0.75	4	7
1	4	6
1.25	3	6
1.5	3	5
1.75	3	5
2	3	4

approximately half the ring axial length (0.01 m). Zero axial offset results in maximum axial stiffness as seen in Fig. 3(*b*).

- The values of an axial offset at which force and stiffness are maximum are independent of number of ring pairs [18].
- Based on this optimized axial offset, the values of other design variables (g, n, $R1$, and $R3$) are estimated.
- Air gap (g) is varied from 0.25 to 2 mm in steps of 0.25 mm to optimize number of ring pairs in the given control volume.
- Optimized value of number of ring pairs (n_{opt}) is determined by varying the rings in the control volume for different air gaps.
- $R1$ is optimized by fixing $R3$ and n_{opt} for different air gaps

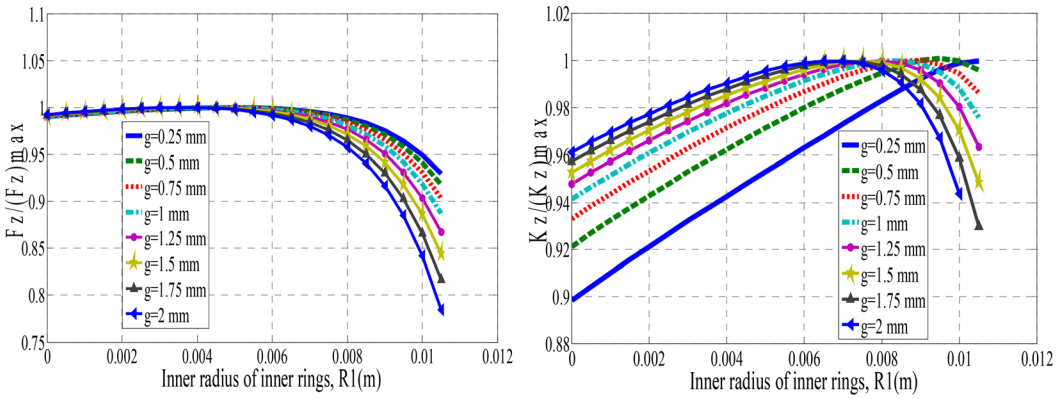

(*a*) (*b*)

Fig. 6 Variation of optimized values of *R*1 for different air gap values for maximum axial (*a*) force and (*b*) stiffness

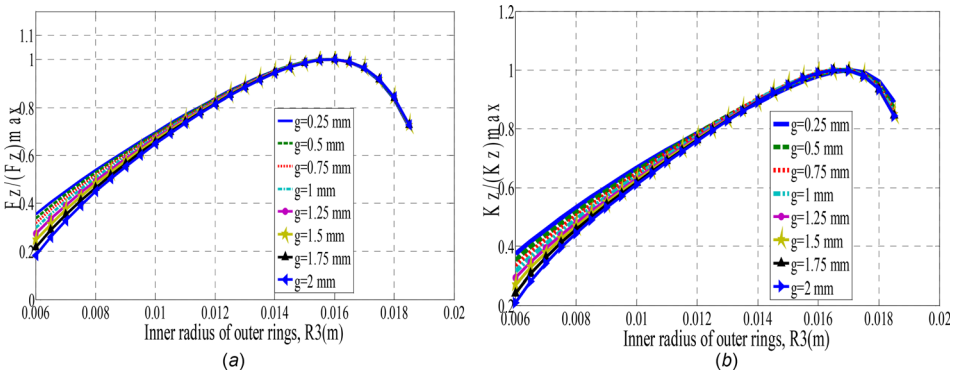

(*a*) (*b*)

Fig. 7 Variation of optimized values of *R*3 for different air gap values for maximum axial (*a*) force and (*b*) stiffness

Table 3 Optimized values of geometrical parameters of PM thrust bearing

Parameters	Optimized values for maximum axial force	Optimized values for maximum axial stiffness
z (m)	0.0025	0
n	4	6
$R1$ (m)	0.004	0.0085
$R2$ (m)	0.015	0.0155
$R3$ (m)	0.016	0.0165
$R4$ (m)	0.02	0.02

- $R3$ is optimized based on the optimized values of z, n, and $R1$ for different air gaps.

Figure 4 presents flow chart detailing steps involved in the optimization carried out using MATLAB code. Axial force and stiffness values for the selected configuration are plotted in Fig. 5 and are listed in Table 2. The results reveal that the optimum values for number of ring pairs at maximum force and stiffness decrease with increase in air gap between outer and inner rings.

The variables, $R1$ and $R3$ (Fig. 4(*b*)) are optimized based on the earlier optimized axial offset values (z_{opt}), and number of rings (n_{opt}). Figure 6 shows the variation of optimized values of $R1$ as a function of air gap for maximum axial force and stiffness. The maximal force and stiffness values are not quite affected up to certain value of $R1$ (shaft radius). This means that inner permanent

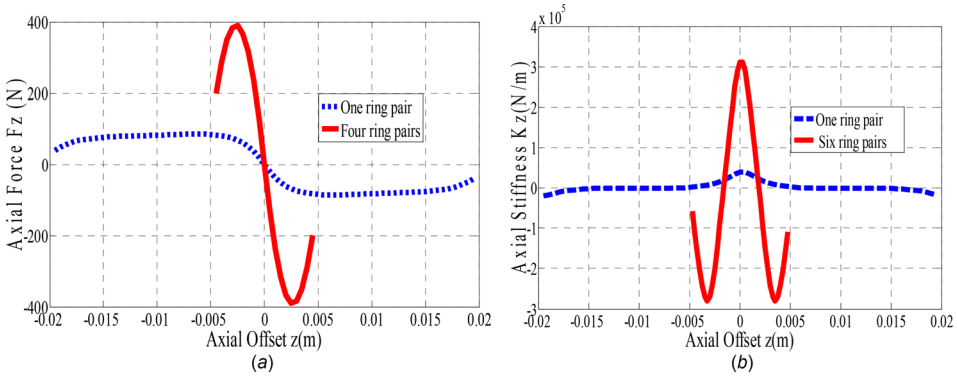

Fig. 8 Force and stiffness values of optimized PM thrust bearing configurations with 1 mm air gap for maximized axial (*a*) force and (*b*) stiffness

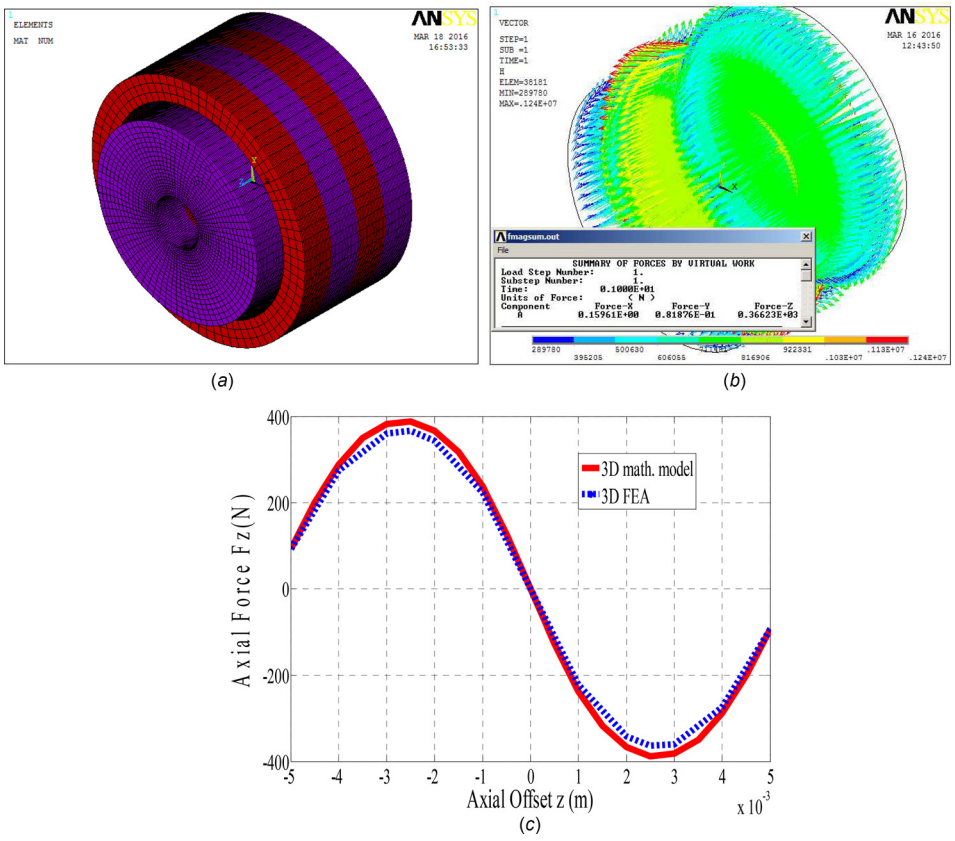

Fig. 9 Optimized configuration FEA results for (*a*) inner and outer rings model, (*b*) maximum force generated on inner rings, and (*c*) comparison of optimized results of 3D mathematical model and 3D FEA results

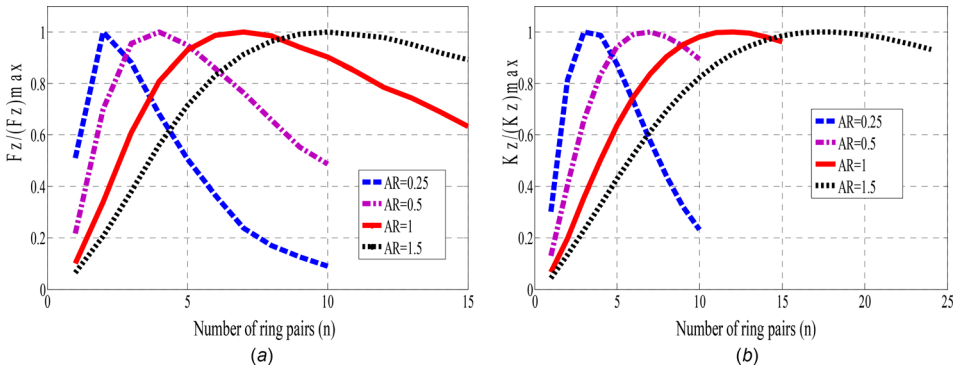

Fig. 10 Optimized values of number of ring pairs for different aspect ratios with respect to maximum axial (*a*) force and (*b*) stiffness

Table 4 Independent of aspect ratio

	Maximum axial force		Maximum axial stiffness	
Aspect ratio (AR)	$(n)_{opt}$	$(n)_{opt}$/AR≈	$(n)_{opt}$	$(n)_{opt}$/AR≈
0.25	2	8	3	12
0.5	4	8	6	12
1	8	8	12	12
1.5	12	8	18	12

magnet rings material does not significantly contribute to axial force and stiffness values and designer can increase the shaft radius up to the critical value in the control volume. However, further increase in the radius causes abrupt change in the maximal force and stiffness values. It is observed that, air gap predominantly depends on $R1$ at maximum stiffness compared to force. Optimization of $R3$ is carried out in similar manner. Once the number of ring pairs (n) and shaft radius ($R1$) are optimized for maximal force and stiffness values, influence of $R3$ (inner radius of outer rings) becomes critical. The variations of axial force and stiffness values with respect to $R3$ for air gap variations are presented in Fig. 7. Results show that, force and stiffness values are maximum at 0.016 and 0.0165 m of $R3$, respectively, with

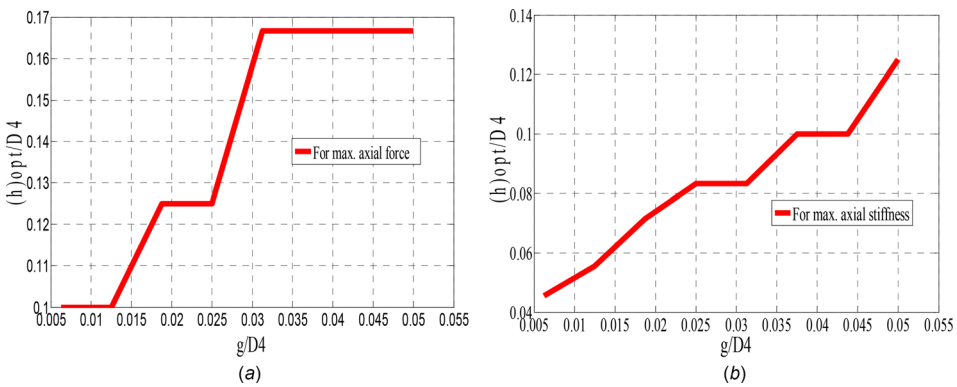

Fig. 11 Optimal magnet thickness as a function of air gap for maximum axial (*a*) force and (*b*) stiffness

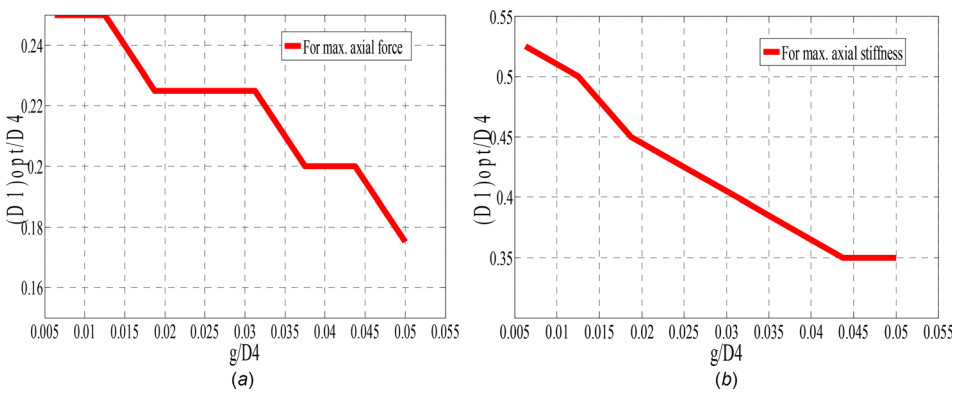

Fig. 12 Optimum value of inner diameter of inner rings as a function of air gap for maximum axial (*a*) force and (*b*) stiffness

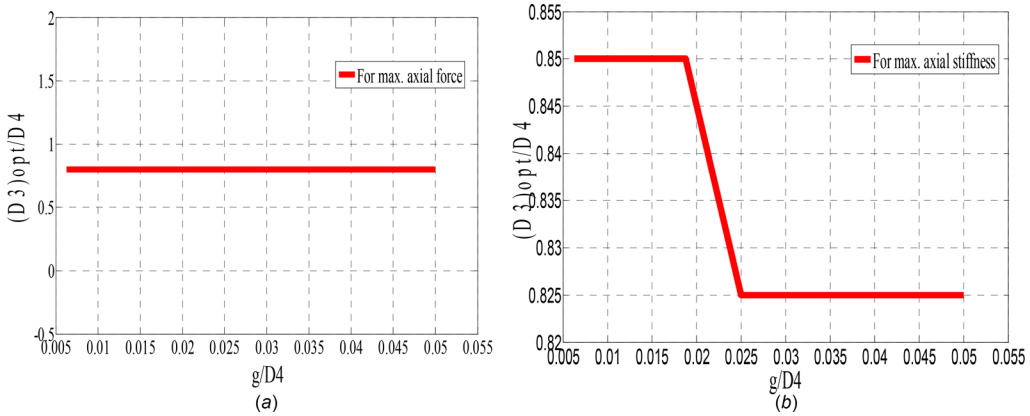

Fig. 13 Optimum value of inner diameter of outer rings as a function of air gap for maximum axial (*a*) force and (*b*) stiffness

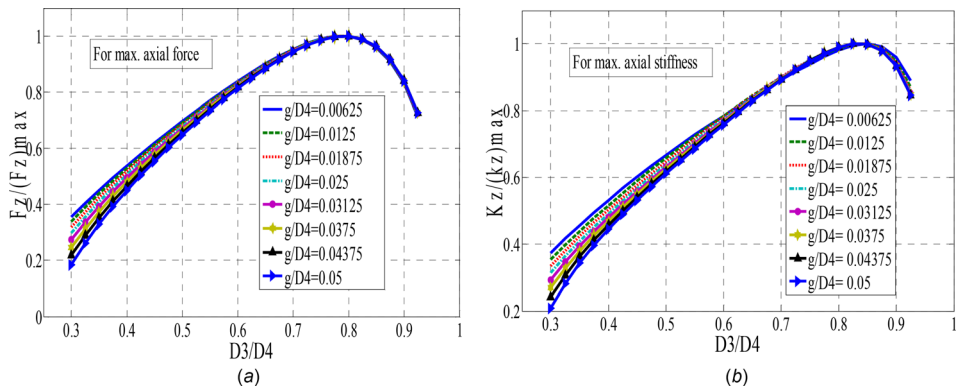

Fig. 14 Variations of optimum value of inner diameter of outer rings for different values of air gap maximum axial (*a*) force and (*b*) stiffness

negligible effect of air gap. The designer should select particular value of $R3$ ($R3_{opt}$) for maximal force and stiffness values. These maximal values are much dependent on $R3_{opt}$ as compared air gap (g).

Optimized geometrical parameters for maximum axial force and stiffness for 1 mm air gap are listed in Table 3. Figure 8 presents the comparison of force and stiffness values of optimized PM thrust bearing with values of one ring pair having aspect ratio of 0.5 at 1 mm air gap. Axial force and stiffness estimated in the optimized configuration is 4.5 (389.38 N) and 7.8 times (311214.1 N/m), respectively, as against one ring pair in a given control volume.

Validation of Optimization Results

The results obtained using proposed optimization method are validated by analysing the optimized PM thrust bearing using 3D FEA in ANSYS (version 13). For the analysis, N35 grade Neodymium Iron Boron (NdFeB) magnet rings are selected with properties as $B_r = 1.2$ T, coercive force $H_c = 868$ kA/m, and relative permeability μ_r ($B_r/\mu_0 H_c$)=1.1. The PM thrust bearing configuration is modeled using 570,970 solid97 elements with 212,196 nodes by polarizing the rings in alternate opposite directions (Fig. 9(*a*)). Solid97 is eight-node 3D magnetic solid element, which is used to model 3D magnetic fields. Magnetic virtual displacement method is used to determine the axial force (Fig. 9(*b*)) exerted by the outer rings on inner. Variation of axial force with an axial offset for optimized configuration using mathematical model in comparison with FEA is plotted in Fig. 9(*c*). It is observed that the axial force values obtained using optimization method are in close agreement (5.7%) with 3D FEA results at their maxima.

Generalization of Optimization Procedure

Optimization of number of ring pairs with respect to maximum axial force and stiffness with different aspect ratios is carried out for the geometrical parameters as listed in Table 1. The aspect ratio of the configuration is varied by selecting different axial length of the cylindrical volume as 0.01, 0.02, 0.04, and 0.06 m resulting in the aspect ratios of 0.25, 0.5, 1, and 1.5, respectively. Figure 10 presents the optimum values of n for maximum axial force and stiffness for different aspect ratios. It is observed that ends of the permanent magnet cylinders make constant contribution to maximal axial force and stiffness values irrespective of aspect ratios of the bearing (Table 4). This observation is in accordance with Moser et al. [20] justifying generalizing of optimization procedure adapted in the present work.

Inline to this fact, the optimization procedure of stack structured PM thrust bearing could be generalized for its direct use in the industry by establishing the relationship between optimized design variables and air gap with respect to volume constraint of bearing outer diameter ($D4$). The variations of optimal design variables with respect to $D4$ such as axial ring thickness ($(h)_{opt} = L/n$), inner diameter of inner rings ($(D1)_{opt}$) and inner diameter of outer rings ($(D3)_{opt}$) with air gap for maximum axial force and stiffness are presented in Figs. 11–13. Further, the optimum values of $D3/D4$ for different values of $g/D4$ for maximum axial force and stiffness are shown in Fig. 14.

Following are the observations made from the generalized plots for the selected range of air gap (0.25–2 mm),

- Optimal value of ring axial thickness increases with air gap with respect to force and stiffness maximizations (Fig. 11).

Table 5 Optimum values of the design variables

PM thrust bearing for maximum axial force	PM thrust bearing for maximum axial stiffness
Fig. 11(*a*) $(h)_{opt}/D4 = 0.125 \rightarrow (h)_{opt} = 0.0075$ m	Fig. 11(*b*) $(h)_{opt}/D4 = 0.083 \rightarrow (h)_{opt} = 0.00498$ m
Fig. 12(*a*) $(D1)_{opt}/D4 = 0.225 \rightarrow (D1)_{opt} = 0.0135$ m	Fig. 12(*b*) $(D1)_{opt}/D4 = 0.425 \rightarrow (D1)_{opt} = 0.0225$ m
Fig. 13(*a*) $(D3)_{opt}/D4 = 0.825 \rightarrow (D3)_{opt} = 0.0495$ m	Fig. 13(*b*) $(D3)_{opt}/D4 = 0.825 \rightarrow (D3)_{opt} = 0.0495$ m

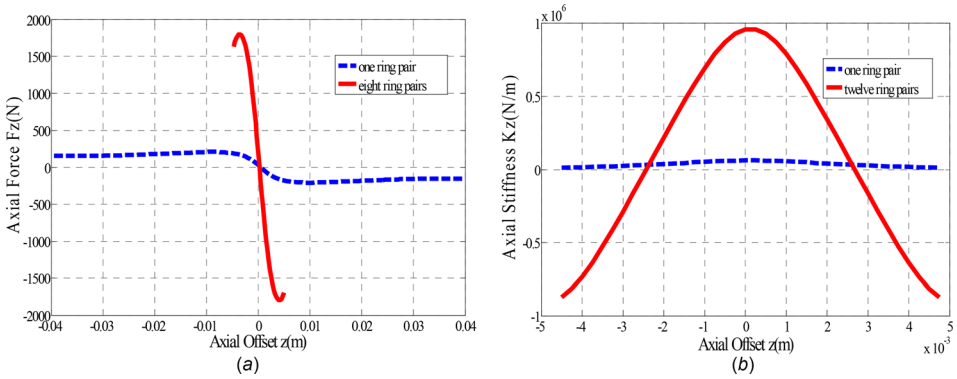

Fig. 15 Optimized PM thrust bearing configuration results for (*a*) axial force versus axial offset (*b*) axial stiffness versus axial offset

- Inner diameter of inner rings (shaft diameter) optimal value decreases with increase in the air gap with respect to force and stiffness maximizations (Fig. 12).
- Optimal value of inner diameter of outer rings is almost constant for the selected range of air gap with respect force maximization whereas shows declining trend between 0.725 and 1 mm for stiffness maxima.

Herewith, guidelines are proposed for using the plots (Figs. 11–13) for optimizing design variables in PM thrust bearing is demonstrated for readers/users:

Permanent magnet thrust bearing with outer dimensions should be lower than $L = 0.06$ m and $D4 = 0.06$ m. The following calculation steps result in an optimized configuration of PM thrust bearing with respect to maximized axial force and stiffness.

(1) The outer diameter of bearing, $D4 = 0.06$ m.
(2) $g = 0.0015$ m and $g/D4 = 0.025$.
(3) Based on $g/D4 = 0.025$, the optimum values of the design variables for configurations with maximum axial force and stiffness are presented in Table 5.
(4) The maximized values of force and stiffness in optimized stack structured PM thrust bearing along with the results of single ring pair in the given control volume are shown in Fig. 15. It is observed that axial force and stiffness generated in the optimized configuration are 8.6 (1794.6 N) and 15.4 (956039.2 N/m) times the results of single ring pair configuration.

Conclusions

Three-dimensional expression for axial force and MATLAB codes are developed to carry out the optimization of stack structured PM thrust bearing for maximum axial force and stiffness in a given cylindrical volume. The results of the optimized configuration are in close agreement with the results of 3D FEA. There is significant increase in the axial force (4.5 and 8.6 times for bearings with AR equal to 0.5 and 1) and stiffness (7.8 and 15.4 times for bearings with AR equal to 0.5 and 1) in the optimized configurations compared to one ring pair. Designer can use either 3D equations or generalized plots directly for optimizing the PM thrust bearing of any geometry. Generalized optimization procedure representing the variation of optimized design variables with respect to air gap is useful for the optimization of PM thrust bearing in a given cylindrical volume which comes handy for industrial practices.

Acknowledgment

Authors thank Vision Group on Science and Technology, Department of Information Technology, Biotechnology and Science and Technology, Bengaluru, Karnataka, India, for supporting the envisaged research vide Grant No. VGST/K-FIST (L1) (2014–2015)/2015–2016, GRD-385. Authors also acknowledge the support provided by KLS Gogte Institute of Technology, Belagavi; ME Department of National Institute of Technology Karnataka, Surathkal and Propulsion Division of National Aerospace Laboratories, Bengaluru for carrying out the research work.

Nomenclature

$\mathbf{B_r}$ = component of the magnetization residual magnetism induction density vector J, T
F_z = axial force, N
H_c = coercive force, A/m
K_z = axial stiffness, N/m
μ_r = relative permeability
μ_0 = absolute magnetic permeability, H/m

References

[1] Sotelo, G. G., Andrade, R., and Ferreira, A. C., 2007, "Magnetic Bearing Sets for a Flywheel System," IEEE Trans. Appl. Supercond., **17**(2), pp. 2150–2153.
[2] Fang, J., Le, Y., Sun, J., and Wang, K., 2012, "Analysis and Design of Passive Magnetic Bearing and Damping System for High-Speed Compressor," IEEE Trans. Magn., **48**(9), pp. 2528–2537.
[3] Bekinal, S. I., Anil, T. R., Kulkarni, S. S., and Jana, S., 2014, "Hybrid Permanent Magnet and Foil Bearing System for Complete Passive Levitation of Rotor," 10th International Conference on Vibration Engineering and Technology of Machinery, Sept. 9–11, University of Manchester, Manchester, UK, pp. 939–949.
[4] Yonnet, J. P., 1978, "Passive Magnetic Bearings With Permanent Magnets," IEEE Trans. Magn., **14**(5), pp. 803–805.
[5] Yonnet, J. P., 1981, "Permanent Magnetic Bearings and Couplings," IEEE Trans. Magn., **17**(1), pp. 1169–1173.
[6] Delamare, J., Rulliere, E., and Yonnet, J. P., 1995, "Classification and Synthesis of Permanent Magnet Bearing Configurations," IEEE Trans. Magn., **31**(6), pp. 4190–4192.
[7] Paden, B., Groom, N., and Antaki, J., 2003, "Design Formulas for Permanent-Magnet Bearings," ASME J. Mech. Des., **125**(4), pp. 734–739.

[8] Samanta, P., and Hirani, H., 2008, "Magnetic Bearing Configurations: Theoretical and Experimental Studies," IEEE Trans. Magn., **44**(2), pp. 292–300.
[9] Ravaud, R., Lemarquand, G., and Lemarquand, V., 2009, "Force and Stiffness of Passive Magnetic Bearings Using Permanent Magnets—Part 1: Axial Magnetization," IEEE Trans. Magn., **45**(7), pp. 2996–3002.
[10] Bekinal, S. I., Anil, T. R., and Jana, S., 2012, "Analysis of Axially Magnetized Permanent Magnet Bearing Characteristics," Prog. Electromagn. Res. B, **44**, pp. 327–343.
[11] Bekinal, S. I., Anil, T. R., Jana, S., Kulkarni, S. S., Sawant, A., Patil, N., and Dhond, S., 2013, "Permanent Magnet Thrust Bearing: Theoretical and Experimental Results," Prog. Electromagn. Res. B, **56**, pp. 269–287.
[12] Yonnet, J. P., Lemarquand, G., Hemmerlin, S., and Rulliere, E. O., 1991, "Stacked Structures of Passive Magnetic Bearings," J. Appl. Phys., **70**(10), pp. 6633–6635.
[13] Tian, L., Ai, X.-P., and Tian, Y., 2012, "Analytical Model of Magnetic Force for Axial Stack Permanent-Magnet Bearings," IEEE Trans. Magn., **48**(10), pp. 2592–2599.
[14] Marth, E., Jungmayr, G., and Amrhein, W., 2014, "A 2D-Based Analytical Method for Calculating Permanent Magnetic Ring Bearings With Arbitrary Magnetization and Its Application to Optimal Bearing Design," IEEE Trans. Magn., **50**(5), pp. 1–8.
[15] Ravaud, R., Lemarquand, G., Lemarquand, V., and Depollier, C., 2008, "Analytical Calculation of the Magnetic Field Created by Permanent-Magnet Rings," IEEE Trans. Magn., **44**(8), pp. 1982–1989.
[16] Ravaud, R., Lemarquand, G., Lemarquand, V., and Depollier, C., 2008, "The Three Exact Components of the Magnetic Field Created by a Radially Magnetized Tile Permanent Magnet," Prog. Electromagn. Res., PIER, **88**, pp. 307–319.
[17] Ravaud, R., Lemarquand, G., Lemarquand, V., and Depollier, C., 2009, "Discussion About the Analytical Calculation of the Magnetic Field Created by Permanent Magnets," Prog. Electromagn. Res. B, **11**, pp. 281–297.
[18] Bekinal, S. I., and Jana, S., 2016, "Generalized Three-Dimensional Mathematical Models for Force and Stiffness in Axially, Radially, and Perpendicularly Magnetized Passive Magnetic Bearings With n Number of Ring Pairs," ASME J. Tribol., **138**(3), p. 031105.
[19] Lijesh, K. P., and Hirani, H., 2015, "Development of Analytical Equations for Design and Optimization of Axially Polarized Radial Passive Magnetic Bearing," ASME J. Tribol., **137**(1), pp. 1–9.
[20] Moser, R., Sandtner, J., and Bleuler, H., 2006, "Optimization of Repulsive Passive Magnetic Bearings," IEEE Trans. Magn., **42**(8), pp. 2038–2042.
[21] Yoo, S. Y., Kim, W. Y., Kim, S. J., Lee, W. R., Bae, Y. C., and Noh, M., 2011, "Optimal Design of Non-Contact Thrust Bearing Using Permanent Magnet Rings," Int. J. Precis. Eng. Manuf., **12**(6), pp. 1009–1014.